INTERNATIONAL JOURNAL OF OPTIMIZATION IN CIVIL ENGINEERING Int. J. Optim. Civil Eng., 2025; 15(3): 469-484



OPTIMAL DESIGN OF UNPROTECTED STEEL MOMENT FRAMES UNDER FIRE CONDITION

A. Asaad Samani¹, S. R. Hoseini Vaez^{1*,†} and, P. Hosseini²

¹Department of Civil Engineering, Faculty of Engineering, University of Qom, Qom, Iran

²Faculty of Engineering, Mahallat Institute of Higher Education, Mahallat, Iran

ABSTRACT

This study addresses the critical necessity for optimized structural design under fire conditions, where conventional methods often prove inadequate. The research focuses on the optimal design of two three and nine story steel moment-resisting frames, without fireproofing protection. The optimization objectives were to minimize the structural weight while satisfying constraints under critical fire scenarios. The key design constraints included inter-story drift and the demand-to-capacity ratio of structural members. The study employed the Enhanced Vibrating Particles System (EVPS) and the Accelerated Water Evaporation Optimization (AWEO) algorithms. A significant aspect of the investigation involved analyzing various severe fire scenarios to identify which parts of the structures are most vulnerable during a fire event. The results demonstrate the effectiveness of the proposed optimization framework in achieving a lightweight yet resilient structural design that meets regulations under extreme thermal loading.

Keywords: Optimization design; Fire scenario; Structural weight; Unprotected steel moment frame.

Received: 16 August 2025; Accepted: 7 October 2025

1. INTRODUCTION

The optimization of structural design under fire conditions represents a critical frontier in modern civil engineering, moving beyond traditional prescriptive code methods.

^{*}Corresponding author: Department of Civil Engineering, Faculty of Engineering, University of Qom, Oom, Iran

[†] E-mail address: hoseinivaez@qom.ac.ir (S. R. Hoseini Vaez)

Metaheuristic algorithms have become indispensable tools for researchers tackling complex optimization problems in recent years [1–4]. Conventional approaches often rely on passive fire protection, which can be costly and may not account for the actual performance of the structural system during a real fire event. Performance-based design optimization offers a paradigm shift, enabling engineers to create structures that are not only lighter and more economical but also demonstrably resilient in specific fire scenarios. This methodology integrates advanced computational fire modeling with structural analysis and sophisticated optimization algorithms. The objective is to minimizing weight while ensuring that key performance criteria, such as inter-story drift and member capacity, are not exceeded during a fire. This is particularly crucial for unprotected steel structures, which lack inherent fire resistance and whose behavior under elevated temperatures is highly nonlinear and complex. By exploring the global structural response, optimization can identify critical weaknesses and lead to designs that inherently manage fire-induced forces and deformations, ultimately enhancing safety and reliability in a cost-effective manner. The following literature review highlights recent advancements in this field.

Behnam analyzes how special steel structures, which use beams to support columns, behave in a fire. It tested two building models and found that both collapsed in less than three hours during different fire simulations, contrary to what standard safety designs predicted. The study concludes that this common structural design possesses a hidden and critical vulnerability to fire [5]. Behnam evaluates how unconventional steel buildings perform when exposed to real fire conditions. Unlike standard designs, structures with features like setbacks or soft stories were found to have their fire safety ratings reduced by up to 55-67%, failing to meet required standards. The research proposes two solutions: limiting maximum steel temperatures to 415-460°C or increasing fire insulation thickness by 20-25% to ensure adequate safety [6].

The experimental study by Rezaeian and Eghbali examined how key components of specific steel frames behave under fire conditions. They found that critical failure for the main beams occurs at 720°C, while the connecting joints fail at temperatures above 760°C. The research concludes that using higher-grade bolts and thicker plates in these connections significantly improves their ability to withstand fire [7].

According to the numerical analysis by Eslami et al. the performance of bolted splice connections in steel structures under fire was critically examined. Their findings highlight that the gap between beam segments, the length of the splice plates, and developed thermal gradients are pivotal factors governing the connection's failure. The study further established that temperature variations, lateral restraint conditions, and axial stiffness levels profoundly influence the overall fire behavior of the beams in moment-resisting frame [8].

Gernay et al. conducted the research to develop fire fragility functions for assessing the probabilistic vulnerability of steel buildings. Their sensitivity analysis revealed that uncertainties in fire load, compartment geometry, and steel's mechanical properties are the most influential parameters. They also proposed a framework to integrate these functions with annual ignition likelihood, enabling the calculation of yearly column failure probabilities for different building heights [9]. Chaboki et al. investigated a comparative analysis of framed-tube and moment-resisting frame systems under extreme thermal and structural conditions. Their findings demonstrate that thermal expansion in heated beams generates critical forces, pushing exterior columns to their elastic limit at temperatures as

low as 130°C in framed-tube structures. Furthermore, the research establishes that while framed-tube systems exhibit superior fire performance, they suffer more severe damage than moment-resisting frames in a post-fire column collapse scenario [10].

Akbulut et al. evaluated how high temperatures influence the dynamic properties of steel columns and frames. Their sequential thermal and modal analysis of 62 different models demonstrated that natural frequencies consistently decrease as temperatures rise. The study also discovered that temperature fluctuations can alter the mode shapes of certain structural profiles, providing critical data that can enhance structural health monitoring and damage assessment for fire-affected steel structures [11]. Bhattacharjee et al. performed a comparative analysis of the fire resistance of various steel grades, including carbon steel and multiple stainless steel types. Their numerical simulations revealed that most stainless steels, particularly austenitic grades, significantly outperform carbon steel, offering up to four times longer failure times under identical loads. The research concluded that a beam's time to failure in fire is primarily governed by the high-temperature behavior of its material and its loading level, rather than the size of its cross-section [12].

Mortazavi et al. expanded the capabilities of the OpenSees software by integrating new thermal elements, enabling a more robust analysis of structures under fire conditions. Their application of this enhanced tool to a three-story eccentrically braced frame (EBF) demonstrated that EBFs significantly improve a building's fire resistance by delaying collapse. This development paves the way for integrated multi-hazard assessments, such as evaluating a structure's vulnerability to fire following an earthquake [13]. Qureshi et al. applied established probabilistic models to evaluate the reliability of fire-protected steel columns designed according to U.S. prescriptive codes. Their analysis revealed a significant variation in failure probability, finding it highly sensitive to factors like the column's section factor, utilization ratio, and the thermal properties of its insulation data for which is often scarce. The study concludes that incorporating reliability-based analyses into the design process is essential for achieving more consistent safety levels across different structural configurations.

Qin and Mahmoud developed a sophisticated 3D finite element model to analyze the collapse mechanisms of a six-story steel building under different fire scenarios. Their simulations revealed that a fire confined to a corner compartment causes the entire structure to twist and deform laterally, while a fire engulfing the entire first floor leads to a progressive vertical collapse. The study demonstrates that advanced numerical modeling can accurately predict the complex collapse behavior of steel structures during fire events [14]. Other researchers have also conducted additional studies in this field [11–24]. The present study contributes to this field by employing and comparing two advanced metaheuristic algorithms (EVPS and AWEO) for the optimal design of three- and nine-story steel moment frames without fire protection. This research systematically analyzes various critical fire scenarios to identify vulnerable scenario of structure. The primary objective is to minimize the total structural weight while adhering to crucial performance constraints, including interstory drift and member demand-to-capacity ratios under severe thermal conditions.

2. FIRE DESIGN

Fire Design is the engineering practice focused on ensuring a building's structural stability and integrity during a fire for a specified period. Its primary objectives are to prevent catastrophic collapse, allow for the safe evacuation of occupants, and enable firefighting operations. For steel structures, this is particularly crucial as steel rapidly loses strength at high temperatures. Consequently, fire design strategies often involve the application of protective materials like spray-on coatings or intumescent paint to insulate structural members, alongside advanced computational modeling to predict a building's behavior under extreme thermal loads and ensure it meets required safety standards.

2.1. Fire Temperatures

Fire Temperatures refer to the thermal environment a structure is subjected to during a fire, which is the primary driver of material degradation and structural collapse. These temperatures are not constant but follow a time-dependent curve, with standard curves like ISO 834 used for certification and design to provide a consistent benchmark. In real fires, the peak temperatures and duration are highly variable, influenced by factors such as the fire load (amount of combustible material), ventilation conditions, and compartment geometry, leading to scenarios ranging from short, intense fires to long, smoldering ones. Modern performance-based design increasingly uses realistic natural fire curves instead of standard ones to more accurately predict structural behavior and optimize safety measures. The ISO 834 curve [29] is an internationally recognized standard time-temperature relationship used to simulate a fully developed, post-flashover compartment fire in structural fire resistance tests. It is defined by a specific logarithmic equation that starts at ambient temperature and rises rapidly, reaching approximately 842°C at 30 minutes and 945°C at 60 minutes. The formulation of the ISO 834 curve is as follows:

$$T_{\sigma} = 20 + 345\log(8t + 1) \tag{1}$$

2.2. Thermal Calculations

Thermal calculations are a fundamental step in structural fire design, aiming to determine the temperature evolution within structural members exposed to fire. This process involves analyzing the three modes of heat transfer: conduction through the solid material (e.g., steel), convection from the hot gases to the member surface, and radiation from the flames and hot surfaces. The core of this analysis is solving the heat equation, often using advanced finite element software, to model how heat from the fire environment (ISO 834 curve) penetrates the member and any protective insulation. The resulting temperature history of the steel cross-section is the critical first output, which is then used in a subsequent structural analysis to evaluate the member's loss of strength and stiffness, and its overall load-bearing capacity during the fire. Also, can use the Eurocode 3 [29] equations, according to Eqs. (2) to (5), to apply the heat transfer process and calculate the temperature of steel members.

$$\theta_{i} = \theta_{i-1} + (\Delta \theta_{i}) \theta_{o} \tag{2}$$

where, θ_i is the temperature of the member at time step i, θ_{i-1} is the temperature at time step (i-1), θ_0 is the ambient temperature before the fire, $\Delta \theta_i$ is the temperature growth of the unprotected steel member during the time step (Δt) can be calculated by Eq. (3).

$$\Delta\theta_{i} = k_{sh} \frac{\frac{A_{m}}{V}}{C_{a}\rho_{a}} \dot{h}_{net,d} \Delta t \tag{3}$$

where, V is the volume of the steel member per unit length, A_m is the surface area of the member per unit length, (A_m/V) is the section factor of the steel member, C_a is the specific heat of steel, ρ_a is the unit mass of steel, k_{sh} is the correction factor for the shadow effect, Δt is the time interval should not be taken as more than 5 seconds, and $\dot{h}_{net,d}$ is the design value of the net heat flux per unit area can be calculated as Eq. (4):

$$\dot{h}_{net,d} = \varphi \cdot \varepsilon_m \cdot \varepsilon_f \cdot \sigma \left[(\theta_r + 273)^4 - (\theta_m + 273)^4 \right] + \alpha_c \cdot (\theta_g - \theta_m) \tag{4}$$

where, φ is the configuration factor, ε_m is the surface emissivity of the steel taken as 0.8 in this study, α_c is the convective heat transfer coefficient taken as 25 in this study, θ_r is the effective radiation temperature for the fire environment, θ_g is the gas temperature in the vicinity of the fire exposed member, θ_m is the surface temperature of the steel member, ε_f is the emissivity of the fire taken as 1, and σ is the Stefan-Boltzmann constant (approximately $5.67 \times 10^{-8} \text{ W/m}^2 \text{K}^4$).

The shadow effect factor (k_{sh}) is determined using Eq. (5) for I-shaped sections.

$$k_{sh} = 0.9 \times \left(\frac{A_m}{V}\right)_b / \left(\frac{A_m}{V}\right) \tag{5}$$

where $(A_m/V)_b$ is the box value of the section factor.

2.3. Optimization Problem

In this study, the optimization problem can be formulated as Eq. (6):

find
$$\mathbf{X} = \{x_1, x_2, ..., x_n\}$$

to minimize $F_w(\mathbf{X})$
subject to $g_k(\mathbf{X}) \le 0$, $k = 1, 2, ..., N_g$
where $\mathbf{X}_{\min} \le \mathbf{X} \le \mathbf{X}_{\max}$ (6)

where **X** is a vector of variables, F_w (**X**) is the objective function, \mathbf{X}_{max} and \mathbf{X}_{min} are the maximum and minimum limits of design variables, respectively, g_k (**X**) is the k^{th} constraint and N_g is the number of constraints.

The objective function for normalizing the weight of frames without fire protection coating is defined as Eq. (7) and the penalty coefficients are applied to the objective function.

$$F_{w}(\mathbf{X}) = \frac{1}{W_{\text{max}}} \sum_{i=1}^{N_{r}} \rho_{i} A_{i} \sum_{i=1}^{N_{e}} L_{j}$$
(7)

where, N_e is the number of elements, N_r is the number of element groups, ρ_i and A_i are the density of steel and cross-sectional area of the i^{th} group section. L_j is the length of the j^{th} element of the i^{th} group and W_{max} is the maximum weight of the structure.

In this study, the beam-column and column-column dimension ratio, DCR of members, and inter-story drift ratio were considered as the constraints according to Eqs. (8) to (10), respectively:

$$g_{G,j} = \begin{cases} \left(f w_B / f w_C^{bot} \right)_j - 1 \le 0 \\ \left(f w_C^{top} / f w_C^{bot} \right)_j - 1 \le 0 \\ \left(d_C^{top} / d_C^{bot} \right)_j - 1 \le 0 \end{cases}, \quad j = 1, ..., N_m$$
(8)

$$g_{T,j}^{DCR} = DCR_{S,j}^T - 1 \le 0$$
 , $T = T_1, T_2, ..., T_{max}$, $j = 1, 2, ..., N_e$ (9)

$$g_{T,i}^{\Delta H} = \left(\Delta H_{d,i}^{T} / \Delta H_{all,i}^{T}\right) - 1 \le 0 , \quad T = T_{1}, T_{2}, ..., T_{\text{max}}, \quad i = 1, 2, ..., N_{s}$$
 (10)

where, $g_{G,i}$ is the geometric constraint of the j^{th} connection, N_m is the number of connections, fw_B, fw_C^{bot} and fw_C^{top} are the flange width of beam, bottom column, and top column for the j^{th} connection, respectively, d_C^{bot} and d_C^{top} are the depths of the bottom and top columns for the j^{th} connection, respectively. DCR $_{S,j}^{T}$ is the DCR of stress for the j^{th} element at j^{th} temperature. $\Delta H_{d,i}^{T}$ and $\Delta H_{all,i}^{T}$ are the horizontal displacement of the j^{th} story and its allowable value at the j^{th} temperature, respectively, and j^{th} is the number of stories.

3. META-HEURISTIC OPTIMIZATION ALGORITHM

3.1. AWEO Algorithm

In this study, the AWEO [30] was used to perform the optimization problems. The AWEO algorithm is based on the WEO algorithm, but has a higher convergence speed and more appropriate performance than WEO. The WEO process performs in two independent steps. Half of the process is based on the monolayer evaporation step and the other is based

on the droplet evaporation step, while the two steps are performed simultaneously in each iteration for the process of the AWEO algorithm.

3.2. EVPS Algorithm

The EVPS algorithm [31,32] was used for the optimization problem. The implementation process of this meta-heuristic algorithm is as follows:

- 1. First, the initial population in the permissible range is generated by Eq. (11).
- 2. In this algorithm, another parameter called memory parameter is defined which stores the number of memory sizes from the best obtained positions for the population.
- 3. The parameter defined according to Eq. (12) determines the effect of the damping level in the vibration.
- 4. Eventually, the new positions of population are updated by Eq. (13).

$$\mathbf{X}_{j}^{i} = \mathbf{X}_{\min} + random.(\mathbf{X}_{\max} - \mathbf{X}_{\min})$$
(11)

$$D = \left(\frac{iter}{iter_{\text{max}}}\right) - \alpha \tag{12}$$

$$\mathbf{X}_{i}^{j} = \begin{cases}
\left[D.A.rand \ 1 + OHB^{j}\right], \quad A = (\pm 1)\left(OHB^{j} - \mathbf{X}_{i}^{j}\right) & (a) \\
\left[D.A.rand \ 2 + GP^{j}\right], \quad A = (\pm 1)\left(GP^{j} - \mathbf{X}_{i}^{j}\right) & (b) \\
\left[D.A.rand \ 3 + BP^{j}\right], \quad A = (\pm 1)\left(BP^{j} - \mathbf{X}_{i}^{j}\right) & (c) \\
\omega_{1} + \omega_{2} + \omega_{3} = 1
\end{cases}$$
(13)

where, \mathbf{X}_{j}^{i} is the *j*th variable of the *i*th particle; \mathbf{X}_{max} and \mathbf{X}_{min} are the upper and lower bounds of design variables in the search space, respectively; *iter* is the current number of iterations; *iter*_{max} is the total number of iterations and α is a parameter with a constant value; ± 1 used randomly; *OHB*, *GP* and *BP* are determined independently for each of the variables; The coefficients ω_1 , ω_2 and ω_3 are the relative importance for *OHB*, *GP* and *BP*, respectively; *rand*1, *rand*2 and *rand*3 are random numbers uniformly distributed in the [0, 1] range.

4. NUMERICAL EXAMPLES

Two numerical examples were considered for the optimal design of 2D steel frames using EVPS and AWEO algorithms. The modulus of elasticity was assumed 2.001×10^5 MPa to solve problems. The expected yield strength (F_{ye}) of the steel for the columns and beams was considered 397 and 339 MPa, respectively. The beam section list was made by all W-shaped sections, but the column sections were selected as wide-flange sections W8 to W14. The optimization process of examples was performed in 20 independent runs. The number of

population and the maximum number of iterations for each optimization algorithm were selected 60 and 300, respectively. Figure 1 shows the pseudo-code for implementing optimal design of steel moment frames exposed to fire.

Start

Determine the optimization variables.

Select fire scenarios S_1 , S_2 , S_3 for thermal loading of steel moment frames.

Extract temperatures from the ISO-834 time-temperature curve for all fire time steps.

For each scenario i

Compute the thermal loads and apply to the frame for i^{th} scenario.

Implement the linear static and thermal analysis of the frame for i^{th} scenario.

Calculate the strength requirements of members and the violation of DCR for all members in

the i^{th} scenario according to Eq. (9).

Calculate the beam-column and column-column dimension ratio and inter-story drift constraints for i^{th} scenario according to Eqs. (8) and (10), respectively.

Increment i=i+1

End For

Apply penalties for constraint violations and compute.

Calculate the penalized objective function of unprotected two steel moment frames.

End

Figure 1: Pseudo-code for an optimal fire design procedure

4.1. Three story, four bay steel frame

This example considers the optimization problem of a three story frame as shown in Figure 2. Grouping of elements and applied loads for the frame are shown in this Figure. The constant gravity load of $W_1 = 32$ kN/m was applied to the first and second stories and the constant gravity load of $W_2 = 28.7$ kN/m was applied to the roof beams. Figure 3 shows the number of elements. The seismic weights were assumed as 4688 kN for the first and second stories and 5071 kN for the third story. The optimal sections, weight of frame, standard deviation (σ) and coefficient of variation (COV) of weights for three story frame are summarized in Table 1. The fire scenarios for three story frame are shown in Figure 4. Figure 5 shows the convergence curve of the best solution obtained by each algorithm for a three story steel frame.

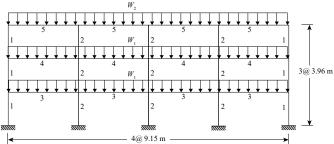


Figure 2: Element grouping and gravity loading of three story frame

TD 11 1	\sim \cdot		1 1 6 1	, ,
Iable I	· (Intima	Leactione and	l weights for thre	a ctary trama
I abic i	. Obullia	i seculons and	weights for time	c story manic

Tuoto 1. Optimai sections and weights for three story frame						
Element group	EVPS	AWEO				
1	W 14 × 176	W 12 × 279				
2	$W 14 \times 176$	$W 14 \times 233$				
3	$W 12 \times 230$	$W 18 \times 175$				
4	$W 18 \times 175$	$W 18 \times 143$				
5	$W 33 \times 152$	$W 18 \times 158$				
Best weight (kN)	450.72	472.00				
Worst weight (kN)	571.64	621.32				
Average weight (kN)	492.18	533.24				
σ of weight (kN)	48.14	58.22				
COV (%)	9.78	10.92				

		B24		B25		B26		B27	
	C11		C12		C13		C14		C15
		B20		B21		B22		B23	
	C6		C7		C8		C9		C10
		B16		B17		B18		B19	
	C1		C2		C3		C4		C5
7777	777,	777	TTT.	7777	777.	7777	<i>777.</i>	7777	777.

Figure 3: Number of elements for three story frame

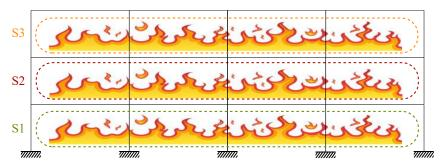


Figure 4: Fire scenarios for three story frame

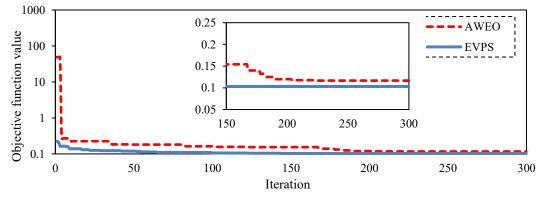


Figure 5: Comparison of the convergence curves for the best solution of algorithms for three story frame

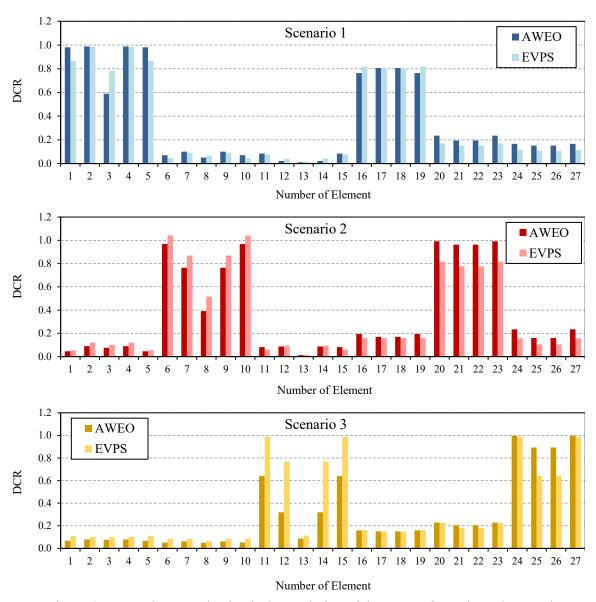


Figure 6: Demand to capacity for the best solution of three story frame in each scenario

According to the convergence curve, the EVPS algorithm performed better than AWEO in finding the optimal answer. Figures 6 show the DCR of elements stress for the best solution of three story frame in each scenario. According to the results this ratio was smaller than unity. Figure 7 compares the inter-story drift ratios to their permitted values for a three story steel frame in each scenario.

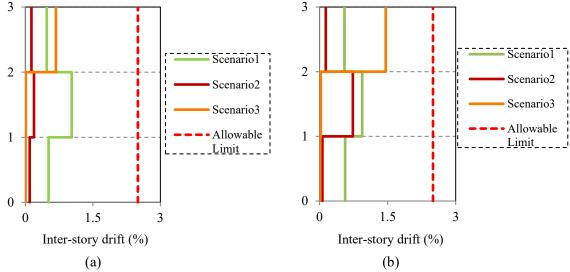


Figure 7: Results of story drift for three story frame of (a) AWEO and (b) EVPS in each scenario

4.2. Nine story, five bay steel frame

A nine-story five-bay steel frame was considered as the second example for optimal fire design problem. Figure 8 shows the grouping of elements and applied loads for the frame. A constant gravity load of $W_1 = 32$ kN/m was applied to the first to eighth stories and a constant gravity load of $W_2 = 28.7$ kN/m was applied to the beams of the roof. The seismic weight for the first story and roof was 1111 kN and 1176 kN, respectively, and for each of the second to eighth stories was 1092 kN. Figure 9 shows the number of elements.

Table 2:Optimal sections and weights for nine story frame

Element group	EVPS	AWEO
1	W 14 × 342	W 14 × 283
2	W 14×370	W 14 × 426
3	W 14 × 176	W 14×257
4	W 14×176	W 14 × 159
5	W 12×230	$W 14 \times 176$
6	W 12×65	$W 14 \times 90$
7	$W 14 \times 132$	W 14×132
8	W 10×100	W 14×90
9	W 14×120	$W 21 \times 93$
10	W 24×103	W 12×170
11	W 21×57	$W 21 \times 44$
12	W 14×48	W 16×50
13	$W 24 \times 94$	$W 27 \times 94$
Best weight (kN)	1180.27	1333.43
Worst weight (kN)	1956.13	2305.33
Average weight (kN)	1688.26	1835.62
σ of weight (kN)	254.11	356.83
COV (%)	17.29	19.99

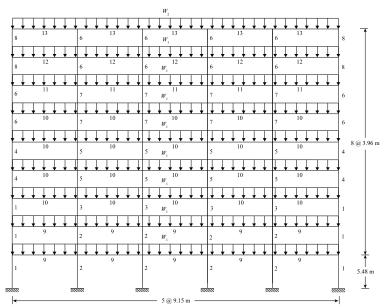


Figure 8: Element grouping and gravity loading of nine story frame

G.10	B95		B96		B97		B98		B99	7
C49		C50		C51		C52		C53		C5-
C43	B90	C44	B91	C45	B92	C46	B93	C47	B94	C4
C37	B85	C38	B86	C39	B87	C40	B88	C41	B89	C4:
C31	B80	C32	B81	C33	B82	C34	B83	C35	B84	C3
C25	B75	C26	B76	C27	B77	C28	B78	C29	B79	C3
C19	B70	C20	B71	C21	B72	C22	B73	C23	B74	C2
C13	B65	C14	B66	C15	B67	C16	B68	C17	B69	C1
C7	B60	C8	B61	C9	B62	C10	B63	C11	B64	Cl
C1	B55	C2	B56	СЗ	B57	C4	B58	C5	B59	Ce
777.	77	mn.	777	7772	777	7777.	777	7777.	7	,,,,,,

Figure 9: Number of elements for nine story frame

The results of optimal sections and the best, worst, average, standard deviation and coefficient of variation of the structure weights are presented in Table 2. The fire scenarios for nine story frame are shown in Figure 10. Figure 11 shows the convergence curve of the best solution obtained by each algorithm for a nine story steel frame. According to the convergence curve, the EVPS algorithm performed better than AWEO in finding the optimal answer. Figures 12 show the DCR of elements stress for the best solution of nine story frame in each scenario. According to the results this ratio was smaller than unity. Figure 13 compares the inter-story drift ratios to their permitted values for a nine story steel frame in each scenario.



Figure 10: Fire scenarios for nine story frame

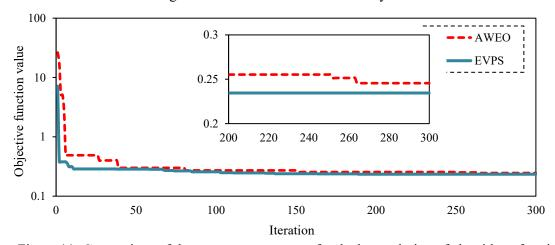
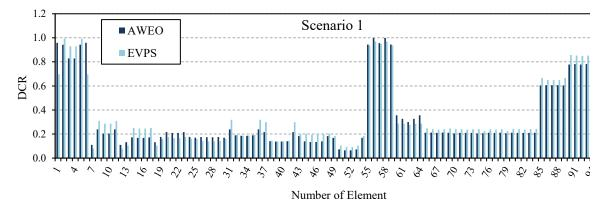


Figure 11: Comparison of the convergence curves for the best solution of algorithms for nine story frame



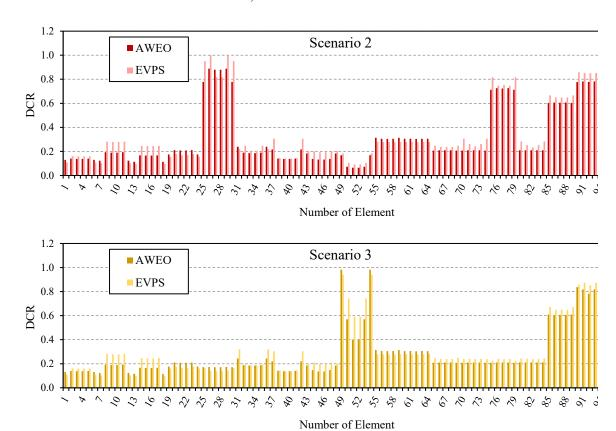


Figure 12: Demand to capacity for the best solution of nine story frame in each scenario

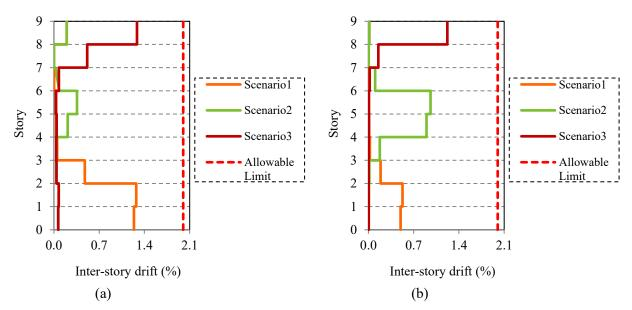


Figure 13: Results of story drift for nine story frame of (a) AWEO and (b) EVPS in each scenario

5. CONCLUSIONS

This research successfully establishes an optimal design of steel moment frames that are both lightweight and resilient to extreme fire conditions. By employing advanced metaheuristic algorithms, the study demonstrates that it is possible to achieve designs that meet stringent safety standards without the need for fireproofing materials.

- Advanced optimization algorithms like EVPS and AWEO can effectively minimize structural weight while maintaining fire resistance.
- Unprotected steel frames can be designed to withstand severe fire scenarios through fire engineering.
- The methodology identifies critical structural vulnerabilities under different fire conditions.
- The approach satisfies both inter-story drift and member capacity requirements under thermal loading.

REFERENCES

- 1. Hoseini Vaez SR, Hosseini P, Fathali MA, Samani AA, Kaveh A. Size and shape reliability-based optimization of dome trusses. Int J Optim Civ Eng. 2020;10:701–14.
- 2. Hoseini Vaez SR, Samani AA, Fathali MA. Optimum performance-based design of unsymmetrical 2D steel moment frame. Soft Comput. 2022;26:5637–59.
- 3. Hoseini Vaez SR, Fathali MA, Samani AA. An approach for optimum performancebased seismic design of 3D steel moment frames. Eng Struct. 2023;301:117248.
- 4. Hosseini P, Kaveh A, Fathali MA, Hoseini Vaez SR. A two-loop RBDO approach for steel frame structures using EVPS, GWO, and Monte Carlo simulation. Mech Adv Mater Struct. 2025;32:605-24.
- 5. Behnam B. Performance of steel moment-resisting beam-supporting column transfer structures under fire. Struct Des Tall Spec Build. 2019;28:1–18.
- 6. Behnam B. A scenario-based methodology for determining fire resistance ratings of irregular steel structures. Adv Struct Eng. 2020;23:89–103.
- 7. Rezaeian A, Eghbali S. Fire response of steel column trees with end-plate connections. J Struct Eng. 2021;147.
- 8. Eslami M, Rezaeian A, Kodur V. Behavior of steel column-trees under fire conditions. J Struct Eng. 2018;**144**:1–15.
- 9. Gernay T, Khorasani NE, Garlock M. Fire fragility functions for steel frame buildings: sensitivity analysis and reliability framework. Fire Technol. 2019;55:1175–210.
- 10. Chaboki M, Heshmati M, Aghakouchak AA. Investigating the behaviour of steel framed-tube and moment-resisting frame systems exposed to fire. Struct. 2021;33:1802– 18.
- 11. Akbulut YE, Altunisik AC, Başağa HB, et al. Elevated temperature effect on the dynamic characteristics of steel columns and frames. Int J Steel Struct. 2021;21:861–82.

- 12. Bhattacharjee T, Nowmi RS, Bhuiyan MH, Ahmed S. Comparison study on characteristic behaviour of hot-rolled beams of carbon steel and stainless steel under standard fire. *Int J Optim Civ Eng.* 2022:1–10.
- 13. Mortazavi SJ, Mansouri I, Awoyera PO, Hu JW. Comparison of thermal performance of steel moment and eccentrically braced frames. *J Build Eng.* 2022;**49**.
- 14. Qin C, Mahmoud H. Collapse performance of composite steel frames under fire. *Eng Struct*. 2019;**183**:662–76.
- 15. Samani AA, Hoseini Vaez SR. Fire resistance and collapse mechanisms of 2D steel moment frames: a numerical study. *J Rehabil Civ Eng.* 2026;**14**:2269.
- 16. Xu Y, Liu M, Zhang T, et al. Application of a dynamo-based intelligent drawing review program in the general code for building fire protection. *Results Eng.* 2025;**27**:106444.
- 17. Kaveh A, Khavaninzadeh N. Nodal ordering of graphs for wavefront optimization using neural network and water strider algorithms. *Iran Univ Sci Technol*. 2024;**14**:647–63.
- 18. Venkatachari S, Kodur VKR. Modeling parameters for predicting the fire-induced progressive collapse in steel framed buildings. *Resilient Cities Struct*. 2023;**2**:129–44.
- 19. Khan AA, Khan MA, Cashell KA, Usmani A. An open-source software framework for the integrated simulation of structures in fire. *Fire Saf J.* 2023;**140**:103896.
- 20. Ye Z, Hsu SC, Wei HH. Real-time prediction of structural fire responses: a finite element-based machine-learning approach. *Autom Constr.* 2022;**136**.
- 21. Jiang L, Jiang Y, Zhang Z, Usmani A. Thermal analysis infrastructure in OpenSees for fire and its smart application interface. *Fire Technol*. 2021;57:2955–80.
- 22. Perković N, Bedon C, Barbalić J, Rajčić V. Study of fire resilience challenges for composite timber-glass walls. *Fire Technol*. 2025:1–29.
- 23. Rathour R, Islam MA, Das A, Alagirusamy R. Protective and mechanical properties of outer shell fabric of thermal/fire protective clothing. *Prog Eng Sci.* 2025;**2**:100120.
- 24. Paknahad M, Hosseini P, Kaveh A, Hakim SJS. A self-adaptive enhanced vibrating particle system algorithm for structural optimization. *Iran Univ Sci Technol*. 2025;**15**:111–30.
- 25. Kaveh A, Eskandari A. Tuned metaheuristic algorithms for optimal design problems with continuous variables. *Iran Univ Sci Technol*. 2025;**15**:259–78.
- 26. Zhang C, Sun G, Wang G, Xiao S. Performance analysis of reinforced concrete frame under fire using multi-scale model. *Results Eng.* 2024;**23**:102402.
- 27. Momin MA, Ahmed KS, Mustafy T, Islam MJ. Damage assessment of materials in a fire-damaged RC building. *Results Eng.* 2024;**24**:102986.
- 28. Mahdavi VR, Kaveh A. Structural damage identification using multi-objective metaheuristic algorithms. *Iran Univ Sci Technol*. 2024;**14**:337–54.
- 29. EN 1993-1-2: Eurocode 3: Design of steel structures Part 1-2: General rules Structural fire design. 1993.
- 30. Kaveh A, Bakhshpoori T. Accelerated water evaporation optimization for discrete skeletal structures. *Comput Struct*. 2016;**177**:218–28.
- 31. Kaveh A, Hoseini Vaez SR, Hosseini P. Enhanced vibrating particles system algorithm for damage identification of truss structures. *Scientia Iranica*. 2019;**26**:246–56.
- 32. Kaveh A, Hoseini Vaez SR, Hosseini P. MATLAB code for an enhanced vibrating particles system algorithm. *Int J Optim Civ Eng.* 2018;**8**:401–14.